ELSEVIER

PII: S0032-3861(98)00178-5

Polymer Vol. 39 No. 26, pp. 6983–6989, 1998

0032-3861/98/$ - see front matter

Simultaneous liquid–liquid demixing and crystallization and its effect on the spherulite growth in poly(ethylene terephthalate)/ poly(ether imide) blends

Hsin-Lung Chen[a], Jenn Chiu Hwang[b,*], Jen-Ming Yang[c] and Rong-Chung Wang[b]

[a]*Department of Chemical Engineering, National Tsing Hua University, Hsin-Chu 30043, Taiwan, Republic of China*

[b]*Department of Chemical Engineering, Yuan Ze University, Nei-Li, Taoyuan, Taiwan, Republic of China*

[c]*Department of Chemical Engineering, Chang Gung University, Kwei-San, Taoyuan, Taiwan, Republic of China*

(Received 23 June 1997; revised 24 October 1997; accepted 6 February 1998)

Poly(ethylene terephthalate) (PET)/poly(ether imide) (PEI) blends were miscible in the melt, but exhibited simultaneous liquid–liquid phase separation and crystallization over a wide range of temperature and composition. The interplay between these two processes is expected to dominate the morphological formation in the blends. In this study, the phase diagram of PET/PEI blend was determined to evaluate the envelop within which liquid–liquid phase separation was operative with crystallization. A UCST phase diagram below 240°C was identified for this system. The effect of liquid–liquid phase separation on the growth of PET spherulites was studied by small-angle light scattering (SALS). Nonlinear spherulite growths were observed for the blends at higher crystallization temperatures of 210°C and 220°C, while the growths were basically linear below 210°C. The nonlinear growth behaviour was discussed based on the competition between spherulite growth and spinodal decomposition.

(Keywords: poly(ethylene terephthalate); poly(ether imide); blend)

INTRODUCTION

Poly(ether imide) (PEI) is an amorphous high-performance polymer with a glass transition temperature (T_g) of 215°C. PEI has been found to form a miscible blend with poly(ethylene terephthalate) (PET) in the melt[1,2]. When PET/PEI blends were cooled to temperatures below the melting points (M.P.), a liquid–liquid phase separation was found to take place simultaneously with the crystallization of PET[2]. The liquid–liquid phase separation occurred through the spinodal decomposition mechanism and the modulated structure was preserved owing to rapid crystallization of PET[2]. A similar morphological feature was observed in an isotactic polypropylene (i-PP)/ethylene-propylene copolymer (EPR) blend, while this system was immiscible in the melt[3,4].

Because of the miscibility in melt and the occurrence of a liquid–liquid phase separation below M.P., PET/PEI blend may exhibit a 'nonequilibrium upper critical solution temperature (UCST) phase diagram' below M.P. The term 'nonequilibrium' is to emphasize that the liquid–liquid phase separation has no equilibrium significance below M.P., since crystallization was the favourable process[5]. But, owing to the nucleation barrier associated with polymer crystallization, spinodal decomposition could precede crystallization and the resultant blend morphology was determined by the competition between these two processes[5].

In this study, further investigations on simultaneous liquid–liquid phase separation and crystallization in PET/PEI blends are presented. The phase diagram of this system will be determined to evaluate the temperature and composition range where these two processes were operative. The effect of liquid–liquid phase separation on the growth behaviour of PET spherulites will be investigated by small-angle light scattering (SALS). The competition between spinodal decomposition and spherulite growth will be discussed based on the observed growth behaviour.

EXPERIMENTAL

PET with a molecular weight of *ca.* 20 000 was obtained from Nan Ya Plastics Co. Ltd, Taiwan. PEI was obtained from General Electric (GE, Ultem 1000), and its molecular weights were $M_n = 12\,000$ and $M_w = 30\,000$.

Blending of PET and PEI was carried out by solution precipitation. PET and PEI were dissolved in dichloroacetic acid at room temperature, yielding a 4 wt% solution. The blends were subsequently recovered by precipitating them in 10-fold excess volume of water. The blends were washed with a large amount of water and then dried *in vacuo* at 100°C for 5 days. It has been reported previously that PET/PEI blends, as precipitated from dichloroacetic acid, were not fully compatible and about 15 min of annealing at

* To whom correspondence should be addressed

280°C was required to homogenize the blends[2]. Therefore, all the samples used in this study had been homogenized by melt-annealing in a d.s.c. at 280°C for 30 min under a nitrogen atmosphere.

Thermal analysis was performed with a TA Instrument 2000 differential scanning calorimeter. The scanning rate was 20°C/min. The morphology of PET/PEI blends was observed by a Carl Zeiss cross-polarized optical microscopy. The sample under study was melted at 280°C for 3 min on a Linkam HFS91 hot stage; it was then quickly transferred to another hot stage equilibrated at the desired crystallization temperature (T_c), where the resultant morphology was observed.

The growths of PET spherulites in the blends were monitored by SALS. The SALS apparatus was similar to the setup employed by Inaba *et al.*[3,4]. A plane-polarized laser beam (He–Ne laser, 20 mW, wavelength $\lambda = 6328$ Å) was used as the incident source. The sample was placed on a Linkam HFS91 hot stage. The H_V scattering were obtained by placing an analyser behind the sample and the patterns were recorded by a CCD video camera connected to a dynamic image analyser (DIA). The sample was first annealed at 280°C for 3 min followed by cooling at *ca.* 70°C/min to the desired T_c where the spherulite growth proceeded. The H_V scattering patterns were recorded at the time intervals of 10 s by DIA, and the spherulite sizes corresponding to different crystallization time periods were calculated from the scattering maxima[10].

RESULTS AND DISCUSSION

Phase diagram of PET/PEI blends

When a crystalline/amorphous blend is cooled from its miscible melt to a crystallization temperature, crystallization of the crystalline component must be accompanied with segregation of the amorphous component. This segregation is driven by crystallization and is called 'liquid–solid phase separation' in contrast to the liquid–liquid phase separation driven by the unstability or the metastability of the liquid solutions. In some rare instances, the binodal curves intersect the equilibrium M.P. depression curve, then liquid–solid phase separation could take place simultaneously with a liquid–liquid phase separation[5–9].

PET/PEI blends have been shown to exhibit simultaneous liquid–liquid phase separation and crystallization below M.P.[2]. It will be further demonstrated here that these two processes were indeed operative over a wide temperature and composition range. *Figure 1* displays the glass transition regions of PET/PEI blends after crystallizing at 200°C for 11 h. A T_g located at *ca.* 180°C is identified and this T_g is rather independent of initial blend composition. Based on the T_g-composition relationship of miscible melt-quenched PET/PEI blends[2], a T_g of 180°C corresponds to the glass transition of the amorphous regions containing 80 wt% PEI. This means that a strong segregation of PEI had taken place upon crystallization of PET. Although the crystallization of PET would invariably reject PEI into the remaining melt and, hence, an accumulation of PEI might take place, it seems quite unlikely that the observed segregation was solely induced by such a liquid–solid phase separation judging from the very high observed PEI composition.

Suppose the segregation of PEI was induced solely by liquid–solid phase separation, such that the PEI content was continuously accumulated in the remaining miscible melt during crystallization, the composition of the miscible amorphous phase may be calculated from the simple mass balance relationship:

$$w_{PEI} = \frac{w^0_{PEI}}{w^0_{PEI} + w^0_{PET} - \Delta h_f/\Delta h^0_f} = \frac{w^0_{PEI}}{1 - \Delta h_f/\Delta h^0_f} \quad (1)$$

where w^0_{PEI} and w^0_{PET} are the initial weight fractions of PEI and PET, respectively, Δh_f is the measured enthalpy of melting, and $\Delta h^0_f = 138$ J/g, the bulk enthalpy of melting. $\Delta h_f/\Delta h^0_f$ gives the weight fraction of PET crystals, i.e. the degree of crystallinity in the blend. *Figure 2* compares the amorphous composition calculated from equation (1) with that evaluated from the observed T_g for 50/50 blend crystallized at various temperatures for 11 h. It can be seen that for T_c higher than 240°C, the calculated compositions are in accord with the observed compositions. On the other hand, the observed PEI composition is always higher than the calculated value for $T_c \leq 240$°C. This disagreement suggests that the observed PEI segregation below 240°C may not be induced simply by liquid–solid phase separation; a liquid–liquid phase separation probably had set in during crystallization.

Figure 3 plots the observed PEI composition against the corresponding T_c. The observed PEI compositions are approximately independent of the initial compositions, and the composition is basically lower at higher T_c. Since all the samples under study had been crystallized for 11 h, it

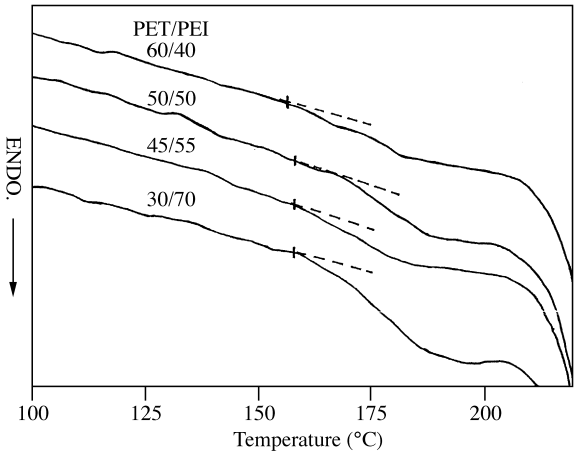

Figure 1 Glass transition regions of PET/PEI blends after crystallizing at 200°C for 11 h

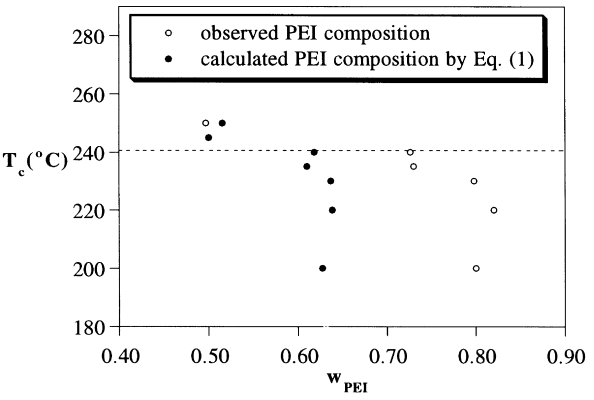

Figure 2 Comparison between the amorphous composition calculated by equation (1) and that evaluated from the observed T_g for PET/PEI 50/50 after crystallizing at various temperatures for 11 h

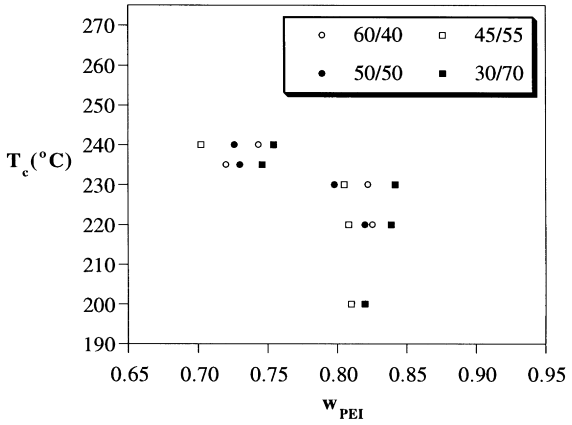

Figure 3 The PEI composition evaluated from the observed T_g *versus* T_c for various PET/PEI blends. The initial PET/PEI compositions are indicated in the figure

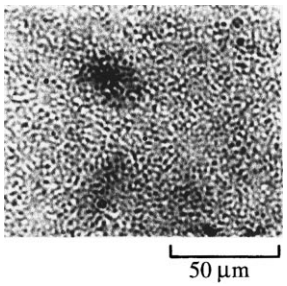

Figure 4 Morphology of PET/PEI 50/50 blend at 220°C. A modulated structure induced by spinodal decomposition is identified

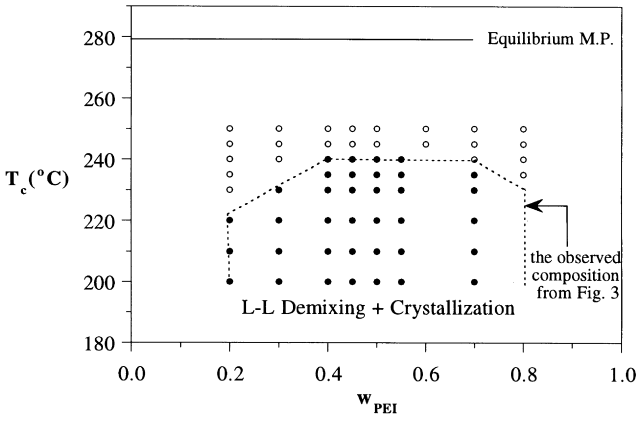

Figure 5 The phase diagram of PET/PEI blend. The open symbol stands for homogeneous state where no phase separation was observed. The filled symbol signifies the observation of both crystallization and spinodal decomposition. Within the region bounded by the dash line, crystallization was found to proceed simultaneously with liquid–liquid phase separation

is reasonable to assume that the observed PEI composition would correspond to the binodal composition of PEI-rich phase after liquid–liquid phase separation. Decrease of PEI composition with increasing T_c would, thus, be an indication for the existence of a UCST type phase diagram. As for the binodal composition of PET-rich phase, the T_g of this phase could not be identified because crystallization should have taken place within this phase owing to high PET concentration. The occurrence of crystallization could further shift the composition into the unstable region and, hence, spinodal decomposition was induced again. Eventually, only the T_g corresponding to the PEI-rich phase was identified.

The occurrence of spinodal decomposition below M.P. can be further demonstrated from the morphology observed by optical microscopy. *Figure 4* displays the bright optical microscopy image for the morphology of PET/PEI 50/50 blend at 220°C. A modulated structure typical of spinodal decomposition is identified. The dark regions in *Figure 4* are either the PET-enriched or PEI-enriched phase. The cocontinuous domains were basically locked in by the crystallization of PET, which is similar to the case of i-PP/EPR blends[3,4]. The temperature and composition range within which liquid–liquid phase separation was coupled with crystallization can be evaluated by observing the resultant morphology for various blend compositions crystallized at different temperatures, as well as comparing the calculated amorphous composition by equation (1) with the observed composition evaluated from T_g. The determined phase diagram is shown in *Figure 5*. *Figure 5* suggests that PET/PEI blend exhibits a nonequilibrium UCST phase diagram with the binodal curve located blow the equilibrium M.P. The blends were miscible over the entire composition range above 240°C. Within the temperature and composition range bounded by the dash line, crystallization was found to proceed simultaneously with liquid–liquid phase separation.

Effect of liquid–liquid phase separation on the spherulite growth

When crystallization of PET is coupled with spinodal decomposition, the crystallization process could be far more complicated than the situation without such a phase separation. Firstly, if spinodal decomposition precedes crystallization, the modulated morphology may be created before the completion of spherulite growth; as a result, the spherulites grow over a space with a periodic composition fluctuation. Although a modulated spinodal morphology may have been formed, the compositions of the two phases may still be changing with one phase continued to enrich the PET content (PET-enriched phase) while the other continued to enrich the PEI content (PEI-enriched phase). This would lead to the spherulites to grow over a space with not only a periodic composition fluctuation, but also with temporal variation of composition. Consequently, a nonconstant rate might be observed throughout the spherulite growth. Kinetically, the growth would proceed favourably along the cocontinuous PET-enriched domains. A continuous enrichment in PET content in these domains should accelerate the growth rate.

Nonconstant growth rate may also arise from the coarsening of spinodal domains during phase separation. As the spherulite growth front advances along the contour of cocontinuous PET-enriched domains, *Figure 6b* shows that the growth path is a distorted one rather than a straight radial route as encountered in the conventional spherulite growth (*Figure 6a*). As the temporal development of spherulite size is measured along the radial direction (i.e. the variation of R with time is measured), the measured growth rate is dependent on the contour of the cocontinuous PET-enriched domains. The spinodal domains are expected to undergo coarsening during spinodal decomposition, the rearrangement of domains would affect the average shape of contour and, subsequently, influence the measured growth rate. If spherulite growth is sufficiently rapid, spinodal domains will be locked in before they have a chance to undergo

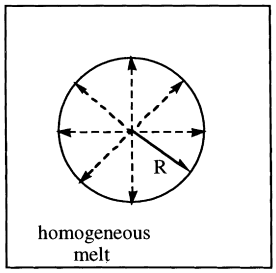

(a)

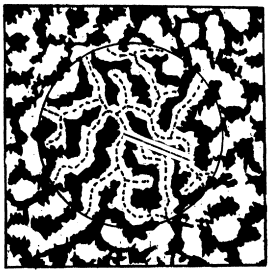

(b)

Figure 6 Schematic representation of the spherulite growth over: (a) a space of homogeneous melt; and (b) a space with modulated domains formed by spinodal decomposition. The dash lines indicate the growth contour. For (b), the bright region is assumed to be the PET-enriched phase. As the growth rate is deduced from the variation of spherulite radius (R) with time, the growth rate is dependent on the growth path. Domain rearrangement changes the average shape of the contour, which could subsequently influence the growth rate

considerable rearrangement[3,4]. In this case, the growth rate remains essentially constant throughout the spherulite growth. On the other hand, if spherulite growth is slow, spinodal domains could undergo considerable rearrangement and composition change; as a result, the growth rate could change with time.

The growth of PET spherulites in the 50/50 blend exhibiting simultaneous spinodal decomposition is shown in *Figure 7*. The bright optical images in this figure were taken with a different method from that used for *Figure 4*. *Figure 4* was taken with the correct focus, but only spinodal morphology could be observed; spherulites could not be identified from the micrograph. On the other hand, the micrographs in *Figure 7* were taken with slight defocus. By doing this, the particles of spherulites can be identified roughly. It was found at $t = 343$ s that the modulated morphology induced by spinodal decomposition has already spread over the space, whereas the spherulites were still small and far before their impingements. This confirmed that the spinodal decomposition, although having no equilibrium significance below the M.P., did take place prior to crystallization. As the modulated morphology was formed far before the completion of spherulite growth, the spherulites grew over the existing modulated domains.

Figure 8 shows the morphology of 50/50 blend observed at different temperatures. The growths of spherulites over existing spinodal domains were observed over the temperature range investigated. No obvious morphological difference in spherulite growth pattern or phase separation pattern was identified. The size of spherulites basically decreases with decreasing T_c, which follows the general rules that nucleation density rises with decreasing T_c.

In order to follow the development of spherulite size, we

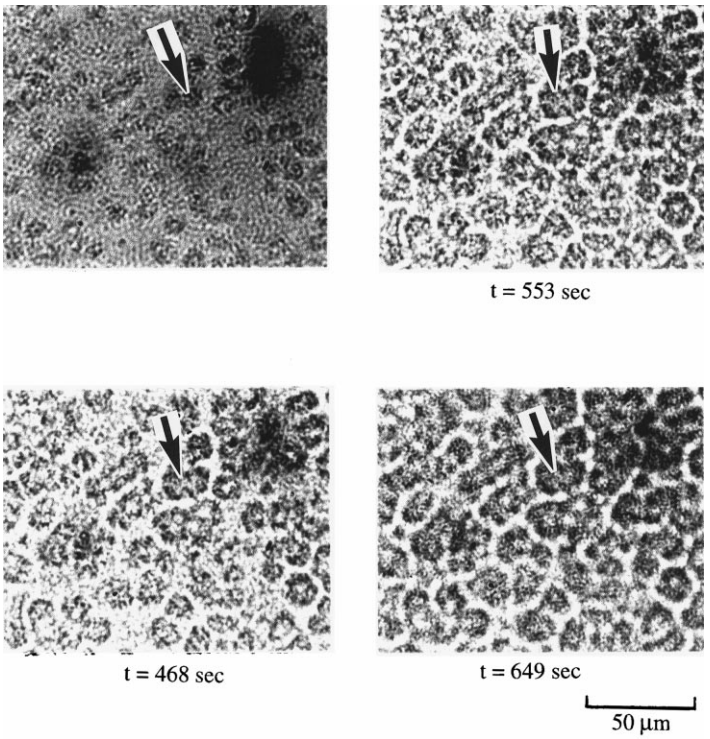

Figure 7 Spherulite growth in PET/PEI 50/50 blend at 220°C. The spherulites are identified as the darker particles (indicated by the arrows). At $t = 343$ s, the modulated morphology induced by spinodal decomposition has already spread over the space, but the spherulites were still small and far before their impingements. This indicated that the spinodal decomposition did take place prior to crystallization

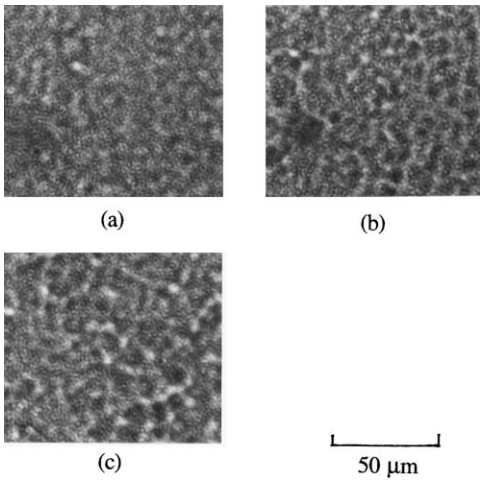

Figure 8 Morphology of 50/50 blend observed at: (a) 190°C; (b) 200°C; and (c) 210°C

used SALS H_V pattern to calculate the average spherulite size for various PET/PEI compositions at different T_cs. *Figure 9* displays the evolution of H_V scattering patterns for PET/PEI 50/50 blend crystallizing at 220°C. The four-leaf H_V patterns indicate the formation of spherulites. The concentration fluctuation arising from spinodal decomposition may lead to a spinodal ring in the V_V scattering pattern[3,4]. However, such a spinodal ring was not observed here, perhaps owing to its weak intensity compared with the background scattering intensity and the interference from the spherulitic scattering.

From the angular position of the scattering maximum in the H_V pattern, θ_{max}, average radius of the spherulites can be determined by[10]

$$R = \frac{4.1}{\frac{4\pi}{\lambda}\sin\left(\frac{\theta_{max}}{2}\right)} \quad (2)$$

The temporal variations of spherulite size at different T_cs are shown in *Figure 10* for PET/PEI 70/30 and 40/60 blends. Below 210°C, the spherulites grew linearly with time while for the two higher T_cs, 210°C and 220°C, the spherulites displayed nonlinear growths. Similar phenomena were also observed for other compositions. These observations indicate that at $T_c < 210$°C the growth rate remained essentially constant, whereas at $T_c \geq 210$°C the growth rate varied with time. The nonlinear growth is characterized by a gradual retardation of growth rate rather than an acceleration. This means the nonlinear spherulite growth, taking place preferentially within the PET-enriched domains, was not owing to the continuous enrichment of PET content associated with phase separation. The nonlinear growth behaviour was alternatively suggested to arise from the rearrangement of the spinodal domains associated with coarsening or from the continuous segregation of PEI content into the growth front, which gradually diluted the PET content as the growth front advanced. The spherulite growths in i-PP/EPR blends over the modulated spinodal domains have been investigated by Hashimoto *et al.*[3,4]. This system exhibited linear growth at a lower T_c of 140°C, but a nonlinear growth at a higher T_c of 145°C. The nonlinear growth behaviour was suggested to relate to the long-range rearrangement of spinodal domains and the segregation of EPR into the growth front.

If the coarsening of spinodal domains attributes to the nonlinear growth behaviour, the growth behaviour is then controlled by the competition between the rate of spherulite

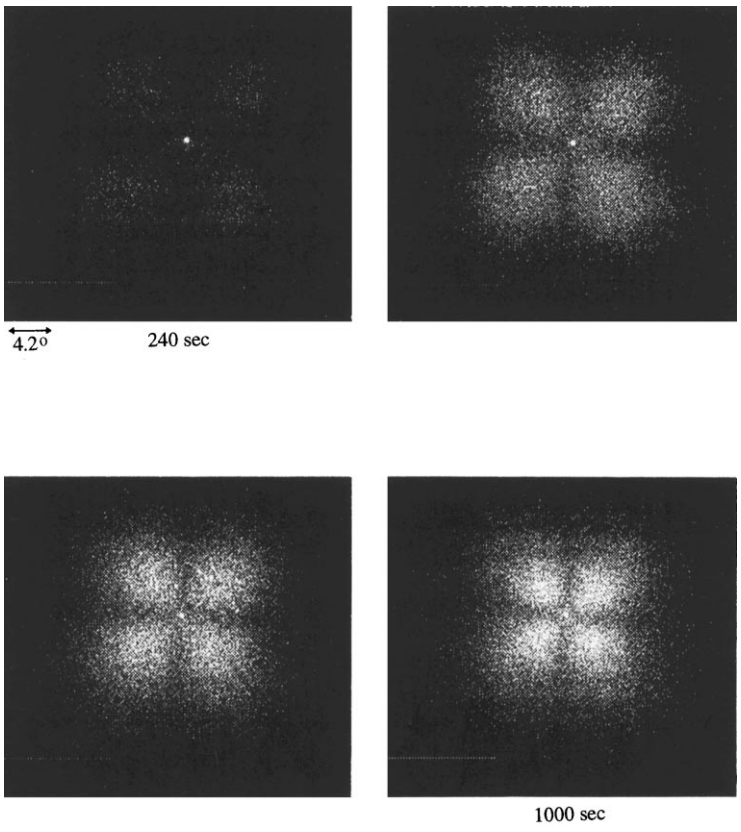

Figure 9 The evolution of H_V scattering patterns for PET/PEI 50/50 blend crystallizing at 220°C for the time periods indicated in the figure

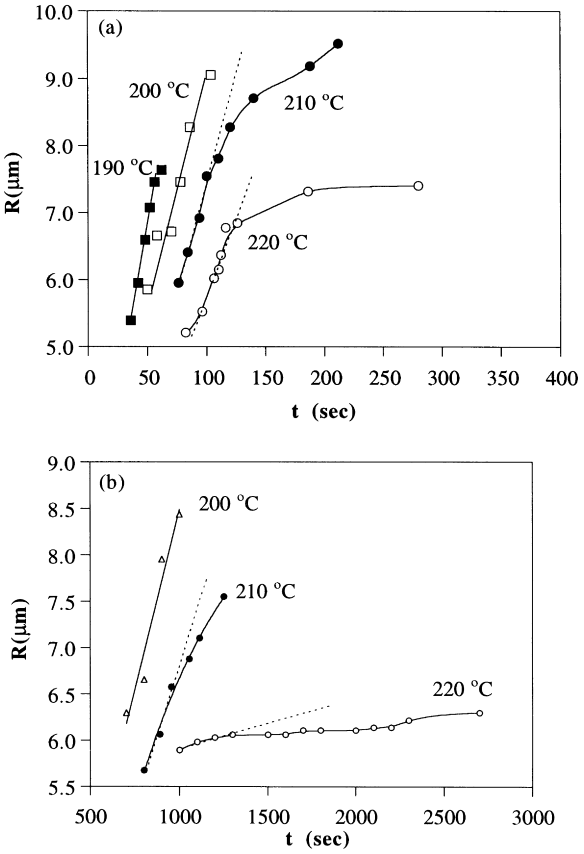

Figure 10 Temporal variations of spherulite size (R) at different T_cs for: (a) PET/PEI 70/30; and (b) PET/PEI 40/60 blends

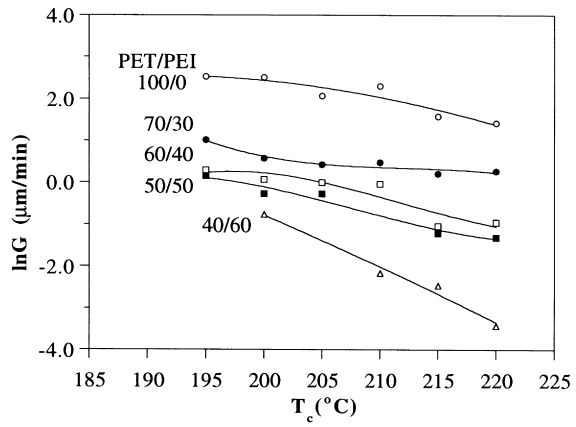

Figure 11 Temperature dependences of growth rate (G) of PET/PEI blends. G decreases with increasing T_c. In spite of the occurrence of spinodal decomposition, G drops with increasing initial PEI composition at a given T_c

growth and spinodal decomposition. Growth rate and spinodal decomposition rate have different temperature dependences. The rates of both processes decrease with increasing T_c in the temperature range investigated, owing to the dominant role of thermodynamic driving force associated with these two processes. *Figure 11* displays the temperature dependence of growth rate. The initial slope in the *R versus t* plot was taken as the growth rate for the temperatures where nonlinear growths were observed. The spherulite growth rate did decrease with increasing T_c. In spite of the occurrence of spinodal decompostion, growth rate still drops with increasing initial PEI composition at a given T_c. If growth rate varies more sensitively with T_c than spinodal decomposition rate, spherulite growth would be depressed by a larger extent than spinodal decomposition when T_c was increased. This appears reasonable because growth rate varies exponentially with temperature, $G \sim \exp(-1/(T_m^0 - T_c))$ (T_m^0 is the equilibrium M.P.), while the spinodal decomposition rate, characterized by the diffusion coefficient $D = -M(\delta^2 f/\partial\phi^2)$ (M, f and ϕ are the mobility, free energy density, and volume fraction, respectively) has the temperature dependence of[11]

$$D \propto |T_c - T_s| T_c \qquad (3)$$

The exponential temperature dependence for growth rate is expected to be more sensitive to temperature change. At low T_c, growth rate was fast so that the spinodal domains were locked-in before they had a chance to undergo considerable rearrangement. As a result, growth rate remained constant throughout the growth process. When T_c was increased, growth rate was depressed by a larger extent than the rate of spinodal decomposition; therefore, compared with at $T_c < 210$°C, the spinodal domains had more time to undergo coarsening before they were locked-in by crystallization. The rearrangement of domains may alter the growth path which in turn influenced the radial growth rate.

Of course, continuous segregation of PEI into the spherulite growth front may be another cause for the observed nonlinear growth. In order to dilute the PET content at the growth front, PEI must be rejected out of the spherulite, which is apparently the largest scale of segregation in semicrystalline polymer blends. A recent study by Runt *et al*. indicated that T_g is the governing factor for the scale of segregation in weakly interacting polymer blends[12]. The scale of segregation decreases with increasing T_g of the amorphous component. PET/PEI blend is a weakly interacting system in that the equilibrium M.P. depression is negligible[13]. Since the T_g of PEI is 140°C higher than that of PET, it seems quite unlikely that PEI could be rejected out of the spherulite during PET crystallization. Small-angle X-ray scattering (SAXS) study is currently underway to evaluate the scale of PEI segregation in PET/PEI blends. The preliminary results showed that the SAXS long period increases with increasing PEI composition, which suggests that PEI is segregated preferentially into interlamellar regions instead of interspherulitic regions. Accumulation of PEI concentration at the spherulite growth front hence did not occur to give rise to the nonlinear growth behaviour. Complete SAXS study for PET/PEI system will be reported in the future publication.

CONCLUSIONS

The phase diagram and the spherulite growth behaviour of PET/PEI blends have been investigated in this paper. PET/PEI blends exhibited a nonequilibrium, UCST phase diagram below 240°C. As a result, crystallization took place simultaneously with a liquid–liquid phase separation. The effect of spinodal decomposition on the growth behaviour of PET spherulites was investigated by SALS. Nonlinear growths were observed at higher T_cs of 210°C and 220°C, while the growths were basically linear below 210°C. The nonlinear growth behaviour was suggested to arise from the coarsening of spinodal domains. At $T_c <$ 210°C, growth rate was fast so that the spinodal domains were locked-in before they had a chance to undergo considerable rearrangement. As a result, growth rate remained essentially constant throughout the growth

process. When the T_c was increased, growth rate was depressed by a larger extent than the rate of spinodal decomposition; therefore, the spinodal domains had more time to undergo rearrangement before they were locked-in by crystallization. The rearrangement of domains may alter the growth path which, in turn, influenced the radial growth rate.

ACKNOWLEDGEMENTS

This work was supported by the National Science Council of the Republic of under grant NSC 86-2216-E-182-001.

REFERENCES

1. Mart'inez, J. M., Eguiaz'abal, J. I. and Naz'abal, J., *J. Appl. Polym. Sci.*, 1993, **48**, 935.
2. Chen, H. L., *Macromolecules*, 1995, **28**, 2845.
3. Inaba, N., Sato, K., Suzuki, S. and Hashimoto, T., *Macromolecules*, 1986, **19**, 1690.
4. Inaba, N., Yamada, T., Suzuki, S. and Hashimoto, T., *Macromolecules*, 1988, **21**, 407.
5. Burghardt, W. R., *Macromolecules*, 1989, **22**, 2482.
6. Tanaka, H. and Nishi, T., *Phys. Rev. Lett.*, 1985, **55**, 1102.
7. Tanaka, H. and Nishi, T., *Phys. Rev.*, 1989, **A39**, 783.
8. Li, Y. and Jungnickel, B. J., *Polymer*, 1993, **34**, 9.
9. Lee, H. K., Myerson, A. S. and Levon, K., *Macromolecules*, 1992, **25**, 4002.
10. Stein, R. S. and Rhodes, M. B., *J. Appl. Phys.*, 1960, **31**, 1873.
11. Inoue, T. and Ougizawa, T. J., *Macromol. Sci. Chem.*, 1989, **A26**, 147.
12. Talibuddin, S., Wu, L., Runt, J. and Lin, J. S., *Macromolecules*, 1996, **29**, 7527.
13. Chen, H. L., Hwang, J. C. and Chen, C. C., *Polymer*, 1996, **37**, 546.